Crystallization heat treatment curves of barium disilicate glass

Curvas de tratamento térmico de cristalização de vidro de dissilicato de bário

DOI:10.34117/bjdv7n8-517

Recebimento dos originais: 07/07/2021
Aceitação para publicação: 23/08/2021

Nícolas Lara
Master's student in Materials Science and Engineering. São Carlos School of Engineering – University of São Paulo (EESC-USP). Avenida João Dagnone, 110 13563-120 - São Carlos, SP – Brazil
nicolaslara@usp.br

Maria Inês Basso Bernardi
Ph.D. in Materials Science and Engineering. São Carlos Institute of Physics – University of São Paulo (IFSC-USP). Avenida João Dagnone , 1100. 13563-120 - São Carlos, SP – Brazil

ABSTRACT
The transformation of glasses into glass-ceramics by heat treatment has been widely studied to increase the toughness of glasses. Barium disilicate is a material that can be toughened this way, greatly increasing its range of applications. To predict the fraction of crystals as a function of heat treatment time and temperature, it is necessary to draw the curves relating these three quantities. For this, data on the nucleation rate and growth rate of barium disilicate crystals were obtained from the literature and processed in order to obtain equations as a function of temperature. These equations were applied to the Johnson-Mehl-Avrami (JMA) equation and integrated in the intervals corresponding to the isothermal treatments, constant cooling from the melting temperature and constant heating from the glass transition temperature, thus obtaining the curves for these three types of heat treatment.

Keywords: glass-ceramics nucleation of crystals in glasses, toughening.

RESUMO
A transformação de vidros em vitrocerâmicas por tratamento térmico vem sendo muito estudada para melhorar a tenacidade de vidros. O dissilicato de bário é um material que pode ser tenacificado dessa forma, aumentando muito sua gama de aplicações. Para prever a fração de cristais em função do tempo e temperatura de tratamento térmico, é necessário traçar as curvas que relacionam essas três grandezas. Para isso, foram obtidos na literatura dados da taxa de nucleação e velocidade de crescimento de cristais do dissilicato de bário e processados de forma a obter equações em função da temperatura. Estas equações foram aplicadas na equação de Johnson-Mehl-Avrami (JMA) e integradas nos intervalos correspondentes aos tratamentos isotérmico, resfriamento constante a partir da temperatura de fusão e aquecimento constante a partir da temperatura de transição vítrea, obtendo assim as curvas para estes três tipos de tratamento.

Palavras-chave: vitrocerâmicas, nucleação de cristais em vidros, tenacificação.

1 INTRODUCTION

The growth of crystals in silicate glasses by heat treatment has been done to manufacture glass-ceramics that are used in several technological applications (LU et al., 2003).

The glass studied in this work is the barium disilicate ($BaO.2SiO_2$). This material has an interesting feature: internal nucleation and crystallization can occur from tempered glass without addition of nucleating agents (CAI et al., 2020), becoming glass-ceramics with a wide range of applications, such as LEDs, sealing of solid fuel cells, and so on (EVARISTO et al., 2020).

1.1 BARIUM DISILICATE

Popularly known as BS2, barium disilicate is part of the $BaO\text{-}SiO_2$ system. Its equilibrium phase diagram is shown in Figure 1:

Figure 1 - $BaO\text{-}SiO_2$ phase diagram

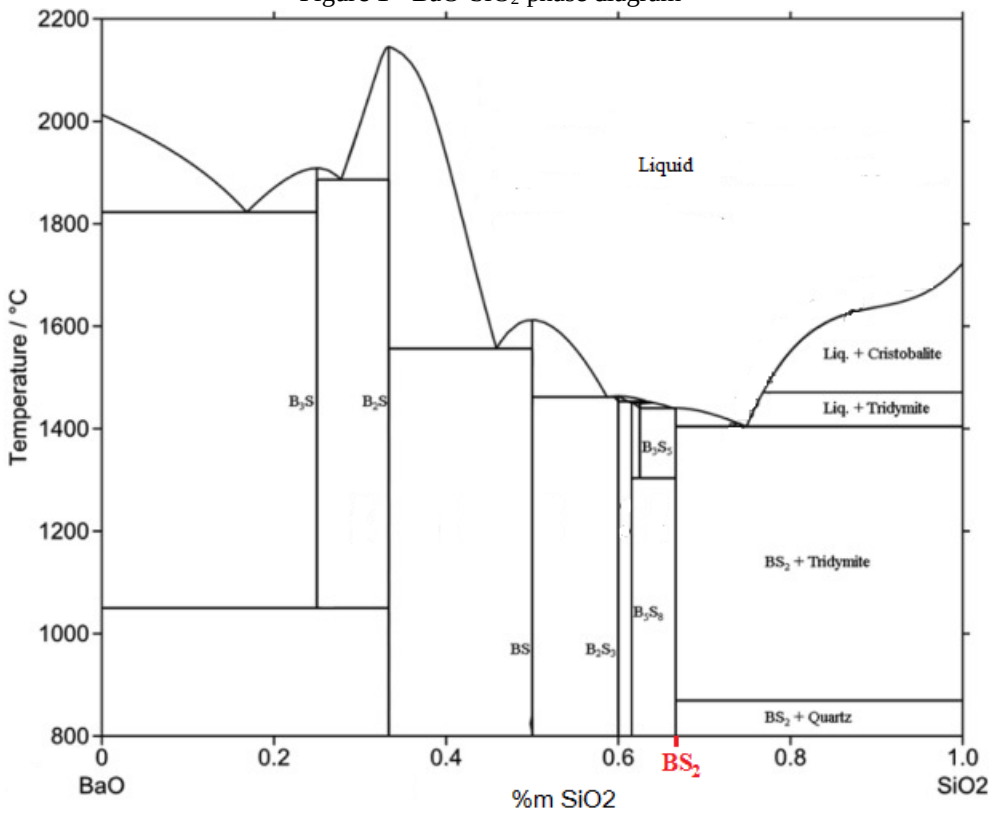

Source: adapted from Zhang and Taskinen (2016)

According to Roth and Levin (1959), BS2 undergoes a reversible polymorphic transformation at 1350 ºC when it cools down. According to Zanotto (1982), BS2 crystals

have a monoclinic structure (h-BS2) at high temperatures and orthorhombic (l-BS2) at lower ones.

In 1965, Macdowell showed that the crystallization of BS2 can be homogeneous, occurring without the addition of nucleating agents. Oehlschlegel (1975) summarizes this process in four steps: 1) classical nucleation, 2) growth of spherulites, 3) monoclinic crystallization and 4) conversion to orthorhombic.

The main physical properties of BS2 (Table 1) in its glassy and crystalline forms were compiled by Zanotto (1982):

Table 1 – Physical properties of barium disilicate.

	Glass	ℓ-BS_2 (ort.)	h-BS_2 (mon.)
ρ ($kg.m^{-1}$)	3740	3770	3730
α ($°C^{-1}$)	91.7×10^{-7}	126.3×10^{-7}	-
V_m ($m^3.mol^{-1}$)	73.14×10^{-6}	72.56×10^{-6}	73.34×10^{-6}
M.W ($kg.mol^{-1}$)	-	273.54×10^{3}	273.54×10^{3}
T_m (°C)	-	-	1420
ΔH_f ($kJ.mol^{-1}$)	-	-	37.0 ±1.0
ΔH_c ($kJ.mol^{-1}$)	-	-	32.0 ±2.0

Source: Zanotto (1982)

In 2016, Rodrigues et al. combined molecular simulations with Raman spectroscopy to study the structure of glassy BS2 at room temperature. Figures 2 and 3 show the distribution of bond angles involving Si-O and Ba-Si-O atoms:

Figure 2 - Distribution of bond angles involving Si and O at 300K

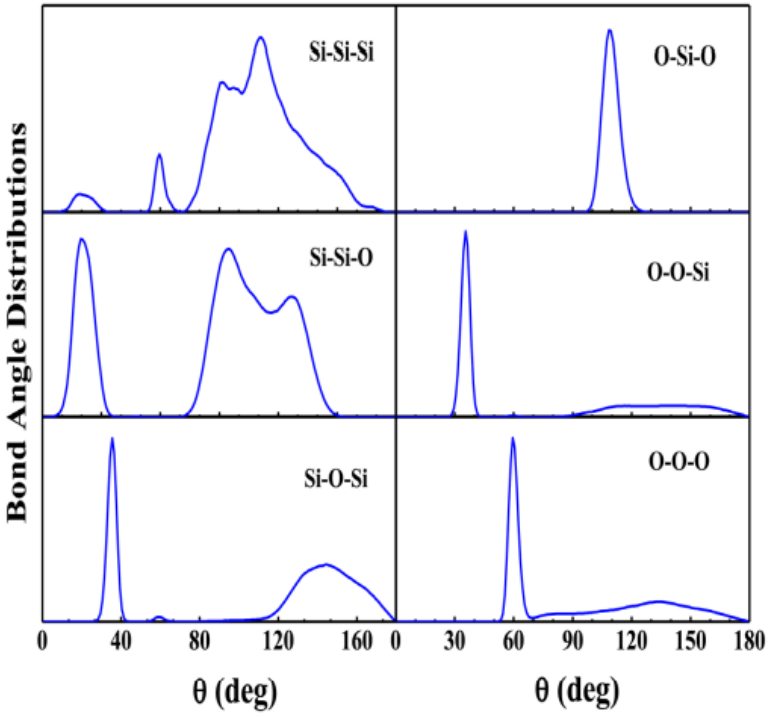

Source: Rodrigues et al. (2016)

Figure 3 - Distribution of bond angles involving Ba, Si and O at 300K

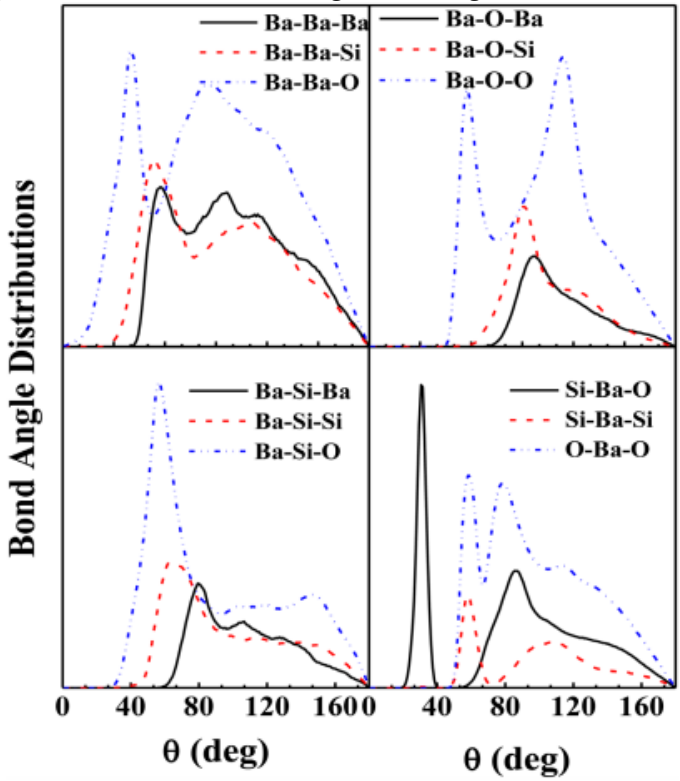

Source: Rodrigues et al. (2016)

Figures 2 and 3 show that the Si atoms are coordinated four times with O and the O–Si–O distribution has a very sharp peak at 109°. This shows the formation of SiO_4

tetrahedrons, just like in silicate glasses. All other angles are very similar to pure silica, with the exception of the Si–Si–Si and Si–O–Si bond angle distributions, which are related to the tetrahedrons connectivity. Compared to pure silica, the presence of Ba in the network causes disruption in the tetrahedral connectivity (RODRIGUES et al., 2016).

Compared to l-BS2, whose rings always have six members, the amorphous phase shows a much wider distribution, showing rings from 3 to 14 times larger. In the crystalline phase, each Si atom will always have 3 bridging oxygens, while in glass form there is a statistical distribution of 1 to 4 (RODRIGUES et al., 2016).

1.2 NUCLEATION KINETICS AND CRYSTAL GROWTH

According to Varshneya and Mauro (2019), the nucleation of crystals in glasses occurs because the atoms are constantly vibrating and moving as a result of the system thermal energy. If each atomic vibration allowed the atom to join together to form a nucleus, the nucleation rate (I) would simply be *nv*, where *n* is the number of atoms per unit volume and *v* is the frequency of atomic vibration. However, there are two barriers that introduce a Boltzmann probability factor for the maximum total rate: the kinetic barrier, ΔE_D, which is the activation energy required for an atom to cross the liquid-core interface, and the thermodynamic barrier, W*, the net free energy change in the system after the formation of a nucleus. Thus, the nucleation rate (I) is:

$$I = nv.\exp\left(\frac{-NW^*}{RT}\right)\exp\left(\frac{-\Delta E_D}{RT}\right) \quad (1)$$

Where N_A is Avogadro's number and R is the ideal gas constant.

Once a critically sized nucleus has formed, crystal growth can occur by packing of atomic layers. According to the Wilson-Frenkel theory and using the Stokes-Einstein relation between the diffusion coefficient and the viscosity (η), the crystal growth rate is:

$$u = \frac{fRT}{3N\pi a^2\eta}\left[1 - \exp\left(\frac{\Delta G_x}{RT}\right)\right] \quad (2)$$

Where *f* is the fraction of surface area with available growth sites, *a* is the distance between two sites and ΔG_x is the free energy of crystallization.

Combining equations (1) and (2), the volume fraction (X) of material crystallized in the glass as a function of heat treatment time can be calculated using the Johnson-Mehl-Avrami (JMA) equation:

$$X = \frac{V_x}{V_0} = 1 - \exp\left(-\frac{\pi}{3} I u^3 t^4\right) \approx \frac{\pi}{3} I u^3 t^4 \qquad (3)$$

Where V_x is the volume of crystallized material and V_0 is the total volume. The right end of the equation is a valid approximation for small values of X.

2 MATERIALS AND METHODS

Barium disilicate crystal nucleation and growth rates data were obtained from the literature (XIA, 2019; RODRIGUES et al., 2018) and approximated by the Least Squares Method in order to obtain their relations as functions of temperature. These relations were replaced in the Johnson-Mehl-Avrami (JMA) equation and integrated in the intervals corresponding to three different heat treatments: isothermal, continuous cooling from melting temperature (T_m) and continuous heating from glass transition temperature (T_g).

3 RESULTS AND DISCUSSION

The nucleation rate was measured by Xia (2019) for the range of 650 to 775 ºC (923 to 1048 K), as shown in Table 2:

Table 2 – Crystal nucleation rates in barium disilicate.

T(K)	I ($mm^{-3}s^{-1}$)
923	3.5 ± 0.2
948	84.0 ± 8.4
973	797.3 ± 94.4
985	1745.2 ± 134.1
998	1246.3 ± 41.2
1011	860.9 ± 41.5
1023	644.9 ± 57.5
1048	239.7 ± 2.9

Source: adapted from Xia (2019)

Plotting the graph, an approximate equation for I as a function of temperature is obtained by the Least Squares Method:

Figure 4 - Nucleation rate as a function of temperature

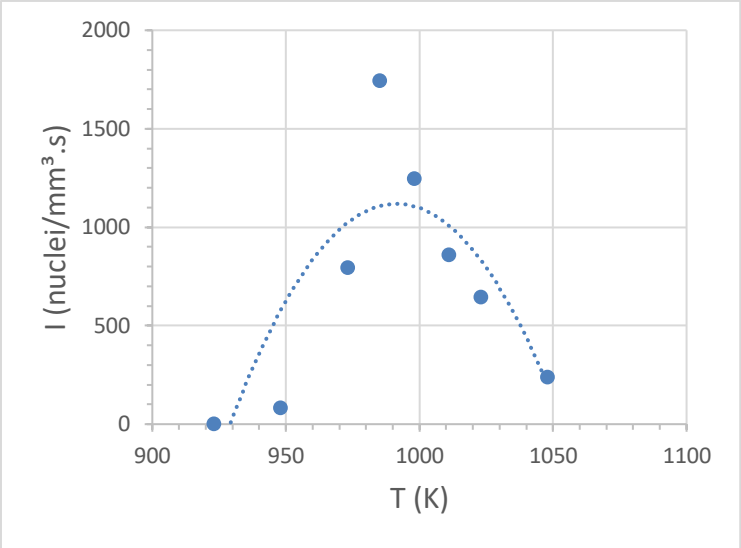

Source: based on Xia (2019)

The best approximation for this data is a degree 2 polynomial. However, this approximation gives negative values of I for temperatures lower than 929 K and greater than 1056 K, which would not make physical sense. Therefore, rates should be considered null for that range. So:

$$I(T) = \begin{cases} -0{,}2875\,T^2 + 570{,}17\,T - 281525 & , \quad 929 \leq T \leq 1056 \\ 0 & , \quad T < 929 \; e \; T > 1056 \end{cases} \tag{4}$$

Crystal growth rates were measured by Rodrigues et al (2018):

Table 3 - Growth rates of barium disilicate crystals

T (K)	u (mm/s)	T (K)	u (mm/s)
983	$5{,}83 \times 10^{-9}$	1073	$3{,}66 \times 10^{-6}$
993	$1{,}58 \times 10^{-8}$	1098	$1{,}50 \times 10^{-5}$
1003	$3{,}50 \times 10^{-8}$	1123	$3{,}24 \times 10^{-5}$
1013	$8{,}17 \times 10^{-8}$	1148	$1{,}36 \times 10^{-4}$
1023	$1{,}75 \times 10^{-7}$	1173	$2{,}41 \times 10^{-4}$
1048	$8{,}51 \times 10^{-7}$	1198	$8{,}86 \times 10^{-4}$

Source: adapted from Rodrigues et al (2018)

Plotting this data into a monolog chart:

Figure 5 - Growth rate as a function of temperature

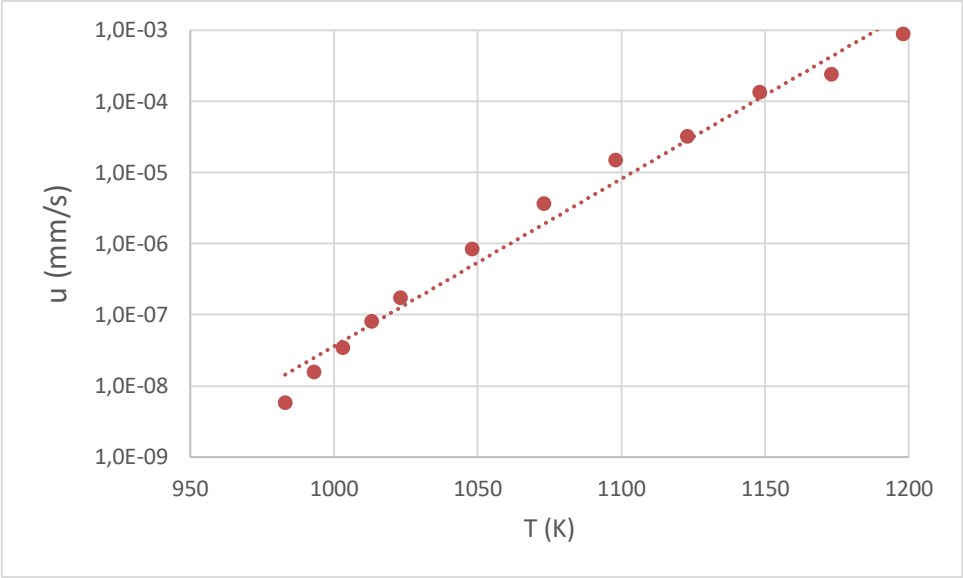

Source: based on Rodrigues et al (2018)

The crystal growth rate function is obtained:

$$u(T) = 10^{-31}\exp(0{,}0542\ T) \qquad (5)$$

Where *u* is given in mm/s and T in Kelvin. It is interesting to plot both curves on the same graph to see how these quantities behave along the analyzed range.

Figure 6 - Nucleation and growth rates as functions of temperature

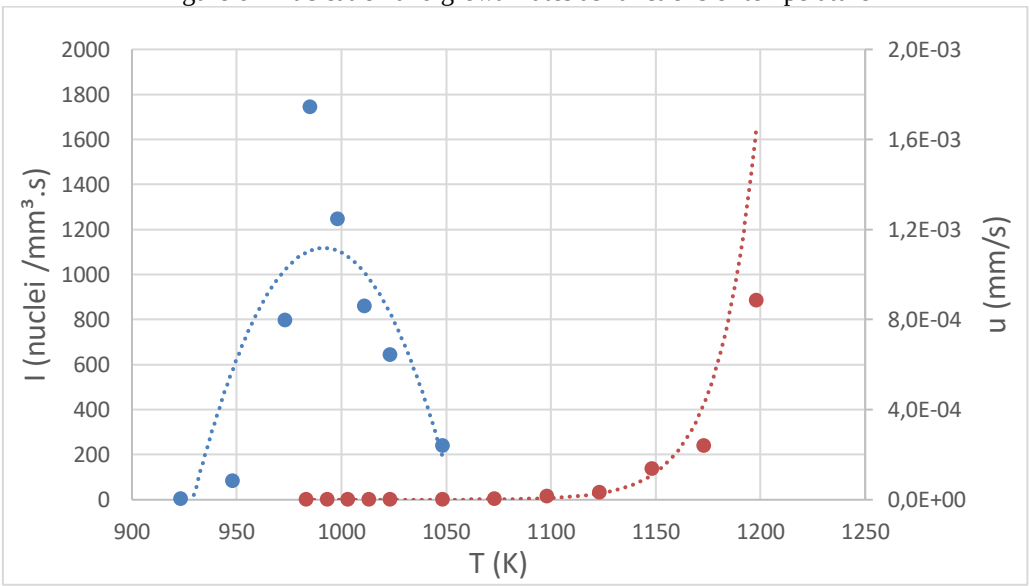

Source: based on Xia (2019) and Rodrigues et al (2018)

Figure 6 shows that the maximum nucleation rate occurs at a much lower temperature than the maximum growth rate. This difference will be important when comparing different heat treatments.

3.1 ISOTHERMAL TREATMENT

The Time Temperature Transformation (TTT) curve for isothermal heat treatments can be obtained by solving the JMA equation (3) for the time:

$$t = \left(\frac{3 \ln\left(\frac{1}{1-X}\right)}{\pi I u^3} \right)^{1/4} \quad (6)$$

And replacing the expressions for the nucleation (4) and growth rates (5):

$$t = \left(\frac{3 \ln\left(\frac{1}{1-X}\right)}{\pi[-0{,}2875\ T^2 + 570{,}17\ T - 281525].[10^{-31} \exp(0{,}0542\ T)]^3} \right)^{1/4} \quad (7)$$

The time (t) that a volumetric fraction (X) is crystallized in BS2 when performing an isothermal treatment can be calculated.

For a measurable crystallized fraction threshold of X = 10^{-3}, the isothermal curve is obtained by substituting this value into equation (6) and plotting the T x t graph:

Figure 7 – TTT curve for a crystallized fraction threshold of 10^{-3}

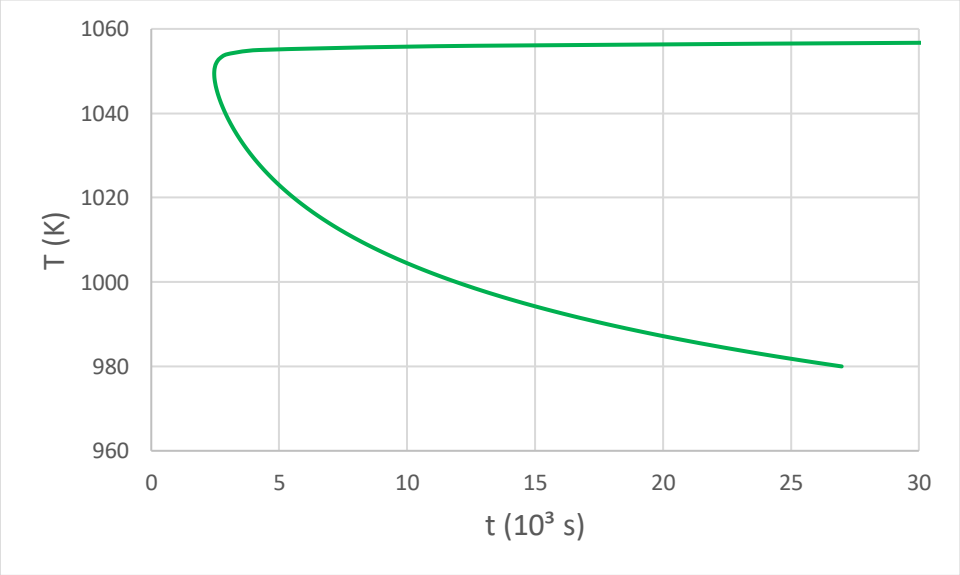

Source: original results based on Xia (2018) Rodrigues et al. (2018), and Varshneya and Mauro (2019)

The curve is similar in shape to the one presented by Varshneya and Mauro (2019) for inorganic glasses. It is asymptotic at temperatures where the nucleation rate reaches zero, as predicted in theory. The curve nose represents the temperature where the isothermal treatment would reach the crystallized fraction threshold in the shortest time. In this case, a 1050 K treatment for 2500 seconds.

The critical rate of nucleation (q_c) can be determined as the slope of the line tangent to the curve nose:

$$q_c = \left(\frac{dT}{dt}\right)_c = \frac{\Delta T_n}{t_n} = \frac{1693-1050}{2500} = 0{,}26\ K/s \qquad (8)$$

This means that for any heat treatment starting from T_m, with a constant cooling rate above 0.26 K/s, there will be no detectable fraction of crystals in the glass (VARSHNEYA and MAURO, 2019).

3.2 CONSTANT COOLING TRANSFORMATION (CCT)

To trace the Constant Cooling Transformation (CCT) curve for constant rate cooling starting on T_m, the variables in the JMA equation (3) must be changed, replacing t by T, isolating the cooling rate and integrating from T_m to the temperature T_x where the volumetric fraction of crystals reaches X:

$$q(Tx) = \left[\frac{4\pi}{3\,X}\int_{Tm}^{Tx} I(T)\left(\int_{Tm}^{Tx} u(T)dT\right)^3 dT\right]^{1/4} \qquad (9)$$

As shown in the deduction of equation (4), the nucleation rate is zero between T_m and 1056 K, so the integration interval of equation (9) must be from 1056 K to T_x. which is the range where there will be both nucleation and crystal growth.

Substituting the expressions for I(T) and u(T) in equation (9):

$$q(Tx) = \left[\frac{4\pi}{3\ 10^{-3}}\int_{1056}^{Tx}(-0{,}2875\ T^2 + 570{,}17\ T - 281525)\left(\int_{1056}^{Tx} 10^{-31}\exp(0{,}0542\ \mathrm{T})dT\right)^3 dT\right]^{1/4} \qquad (10)$$

And solving the integrals:

$$q(Tx) = \left[2{,}63.10^{-8}(e^{-0{,}0542\,Tx} - 6{,}37.10^{39})^3.(-0{,}14375\,T_x^3 + 285\,T_x^2 - 28125\,T_x - 3{,}0.10^8)\right]^{1/4} \quad (11)$$

The expression for the cooling rate as a function of T_x is determined.

The total heat treatment time for each rate can be determined by isolating the time in the cooling rate definition equation:

$$q(T_x) = \frac{dT}{dt} = \frac{T_x - T_m}{t_x - 0} => t_x = \frac{T_m - T_x}{q(T_x)} \quad (12)$$

The CCT curve is traced by plotting the graph of T_x versus time:

Figure 8 - CCT curve for cooling starting on T_m

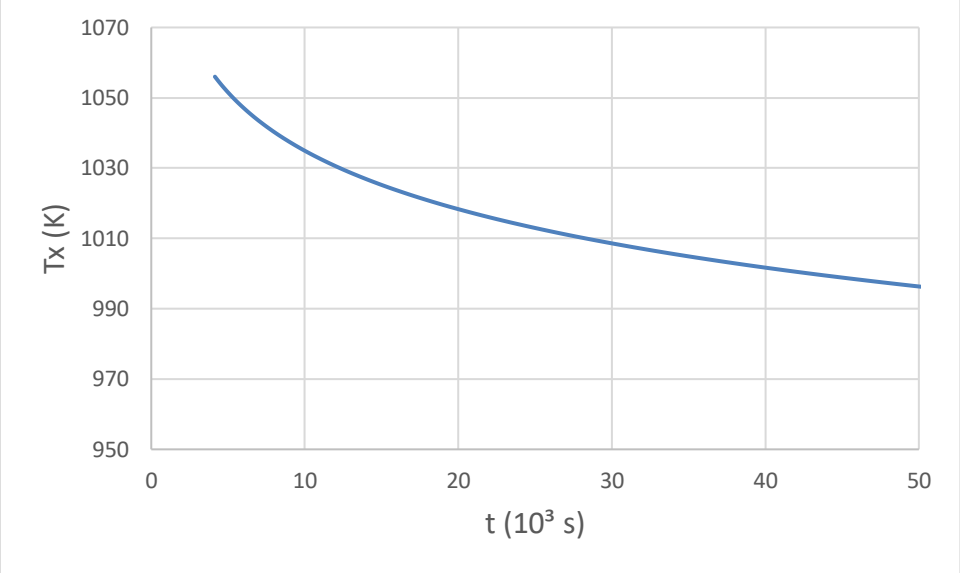

Source: original results based on Xia (2018) Rodrigues et al (2018) and Varshneya and Mauro (2019)

This graph is plotted starting on 1056 K because above that the nucleation rate is zero. However, the time is counted from the beginning of the cooling at T_m.

This CCT curve shows that, in order to obtain a measurable crystallized fraction of 10^{-3} at higher temperatures, the cooling time must be shorter. That is, by using faster cooling rates, the glass will reach the crystallinity threshold quickly, and at a higher temperature.

The curve becomes asymptotic as the temperature drops, as the material enters the zone where the growth rate and nucleation rate are very low, until the latter becomes completely null on 929 K, causing the treatment time tent to infinity. In theory, therefore, if the cooling rate is so fast that the glass reaches 929 K without reaching the crystallization threshold, it will no longer reach it.

3.3 CONTINUOUS HEATING TRANSFORMATION (CHT)

For heating at constant rate starting on T_g, the integration limits of equation (9) must be changed from T_g to T_x:

$$q(Tx) = \left[\frac{4\pi}{3\,X}\int_{Tg}^{Tx} I(T)\left(\int_{Tg}^{Tx} u(T)dT\right)^3 dT\right]^{1/4} \quad (13)$$

Substituting the expressions obtained for u(T) and I(T), and knowing that the value of T_g for BS2 is 963 K (RODRIGUES, 2014):

$$q(Tx) = \left[\frac{4\pi}{3\ 10^{-3}}\int_{963}^{Tx}(-0{,}2875\ T^2 + 570{,}17\ T - 281525)\left(\int_{963}^{Tx} 10^{-31}\exp(0{,}0542\ \mathrm{T})dT\right)^3 dT\right]^{1/4} \quad (14)$$

And solving the integrals, the expression for the heating rate as a function of T_x is obtained:

$$q(Tx) = \left[2{,}63.10^{-8}(e^{-0{,}0542\,Tx} - 4{,}65.10^{22})^3.(-0{,}14375\ T_x^3 + 285\ T_x^2 - 28125\ T_x - 1{,}5.10^8)\right]^{1/4} \quad (15)$$

In the same way as done for cooling, the heat treatment time can be determined by setting the heating rate:

$$q(T_x) = \frac{dT}{dt} = \frac{T_x - T_g}{t_x - 0} \Rightarrow t_x = \frac{T_g - T_x}{q(T_x)} \quad (16)$$

Finally, the CHT curve is the plot of T_x versus time:

Figure 9 - CHT curve for heating starting on T_g

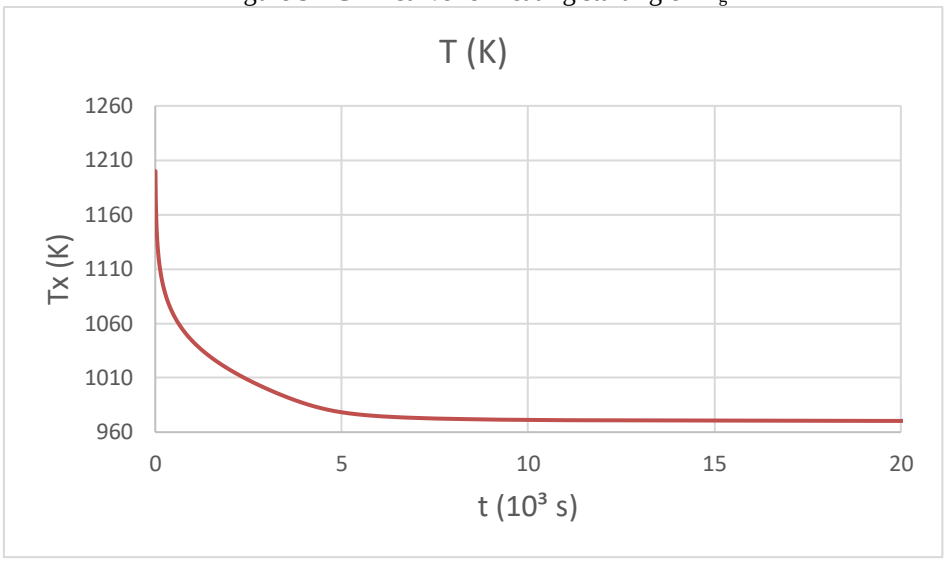

Source: original results based on Xia (2018) Rodrigues et al (2018) and Varshneya and Mauro (2019)

The CHT curve shows that the higher the heating rate, the higher the temperature at which the glass reaches the crystallization threshold. For temperatures very close to T_g, the time is very long, that is, the heating rate must be very slow for the crystallization threshold to form at lower temperatures.

3.4 COMPARISON BETWEEN THE THREE CURVES

Plotting the TTT, CCT and CHT curves on the same graph, it's possible to compare the different types of heat treatment:

Figure 10 - Comparison between TTT, CCT and CHT curves

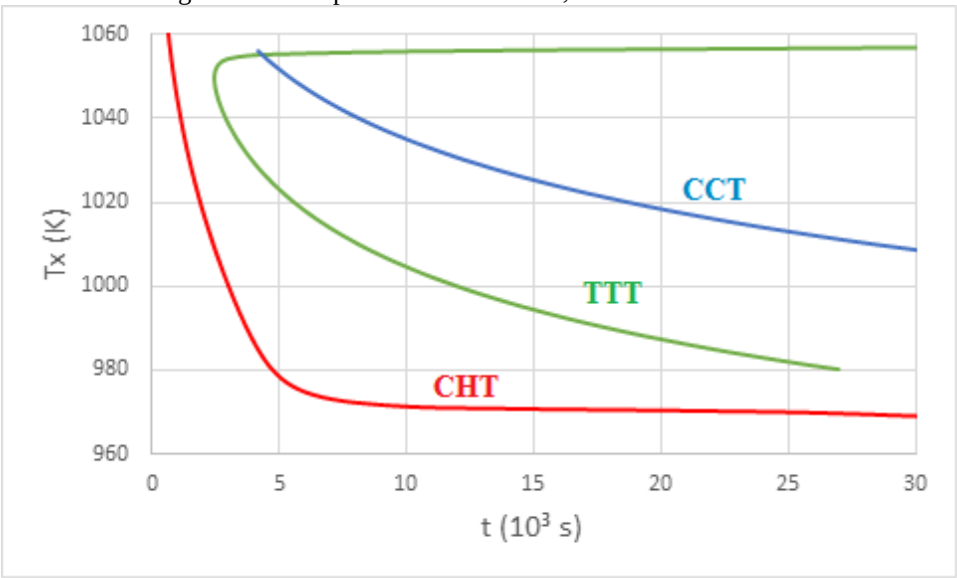

Source: original results based on Xia (2018) Rodrigues et al (2018) and Varshneya and Mauro (2019)

Figure 10 shows that heating from T_g is the treatment in which the crystallization threshold is reached quickly. This is because the maximum nucleation rate occurs at a lower temperature than the maximum growth rate (Fig. 4), therefore the material begins to heat in a region where the crystallization rate is high and then reaches a range where the growth rate is also high.

Figure 4 also explains why the isothermal treatments are not as fast: because there is no temperature at which both the crystallization rate and the growth rate are sufficiently high.

For continuous cooling, the treatment is slower because the glass is in a region of null nucleation, passing a long time without crystallization.

4 FINAL REMARKS

The curves obtained show that the thermal treatments are faster in the following order: cooling from T_m. isothermals and heating from T_g. The main reason for this result is that the maximum growth and nucleation rates occur at very different temperatures.

The crystallization heat treatments presented in this paper can be applied for toughening barium disilicate glasses by crystal growth and can be used to predict the crystallization fraction as a function of temperature and treatment time.

ACKNOWLEDGEMENTS

The authors gratefully acknowledge the financial support of the Brazilian research funding agencies FAPESP (under grant number 2013/07296-2 and 2018/07517-2), CNPq (under grant number 405033/2018), PRONEX/FINEP and CAPES (under grant number 88887.607222/2021-00).

REFERENCES

CAI, L.; YOUNGMAN, R.E.; BAKER, D.E.; REZIKYAN, A.; ZHANG, M.; WHEATON, B.; DUTTA, I.; AITKEN, B.G.; ALLEN, A.J. Nucleation and early stage crystallization in barium disilicate glass. Journal of non-Crystalline Solids, vol. 548, p. 120330, nov. 2020. http://dx.doi.org/10.1016/j.jnoncrysol.2020120330

EVARISTO, L.L.; MOULTON, B.J.A.; PIZANI, P.s.; BUCHNER, S. Effect of high pressure on the structure of barium disilicate glass-ceramics. Journal of Non-Crystalline Solids, vol. 550, p. 120380-120387, Dec. 2020. http://dx.doi.org/10.1016/j.jnoncrysol.2020.120380

LU, S.G.; MAK, C.L.; WONG, K.H. Optical studies of transparent ferroelectric strontium–barium niobate/silica nanocomposite. Journal of Applied Physics, vol. 94, p. 3422, 2003. https://doi.org/10.1063/1.1599047

OEHLSCHLEGEL, G. Crystallization of glasses in the system BaO·2SiO2-2BaO·3SiO2. Journal of the American Ceramic Society, vol. 58, no. 3-4, p. 148, Mar. 1975. http://dx.doi.org/10.1111/j.1151-2916.1975.tb19584.x.

RODRIGUES, A.M. Diffusion processes, crystallization and viscous flow in vitreous barium disilicate. 176 f. Thesis (Doctorate) - Course of Science and Engineering of Materials, Federal University of São Carlos, São Carlos, 2014.

RODRIGUES, A.M.; RINO, J.P.; PIZANI, P.s; ZANOTTO, E.D. Structural and dynamic properties of vitreous and crystalline barium disilicate: molecular dynamics simulation and Raman scattering experiments. Journal of Physics D: Applied Physics, vol. 49, no. 43, p. 435301-435312, set. 2016. http://dx.doi.org/10.1088/0022-3727/49/43/435301

RODRIGUES, A.M.; CASSAR, D.R.; FOKIN, V.M.; ZANOTTO, E.D. Crystal growth and viscous flow in barium disilicate glass. Journal of Non-Crystalline Solids, vol. 479, p. 55-61, Jan. 2018. https://doi.org/10.1016/j.jnoncrysol.2017.10.007

ROTH, R.S.; LEVIN, E.M. Phase balances in the subsystem barium disilicate i- dibarium trisilicate. Journal of Research of the National Bureau of Standards, vol. 62, no. 5, p. 193-201, May. 1959. http://dx.doi.org/10.6028/jres.062.034

VARSHNEYA, A.K.; MAURO, J.C. Fundamentals of Inorganic Glasses. 3. ed. Amsterdam: Elsevier, 2019.

XIA, X.; VAN HOESEN, D.C.; MCKENZIE, M.E.; YOUNGMAN, R.E.; GULBITEN, O.; KELTON, K.F. Time-dependent nucleation rate measurements in BaO·2SiO2 and 5BaO·8SiO2 glasses. Journal of Non-Crystalline Solids, vol. 525, p. 119575-119585, Dec. 2019. https://doi.org/10.1016/j.jnoncrysol.2019.119575

ZANOTTO, E.D. The effects of amorphous phase separation on crystal nucleation in baria-silica and lithia-silica glasses. 327 f. Thesis (Doctorate) - Course in Ceramics, Glasses and Polymers, The University of Sheffield, Sheffield, 1982.

ZHANG, R.; TASKINEN, P. Experimental investigation of liquidus and phase stability in the BaO–SiO2 binary system. Journal of Alloys and Compounds, vol. 657, p. 770-776, Feb. 2016. http://dx.doi.org/10.1016/j.jallcom.2015.10.165.